

Development of the Low-Cost PNT Unit for Maritime Applications Using MEMS Inertial Sensors

Michailas Romanovas*, Luis Lanca*, Ralf Ziebold*

*Institute of Communications and Navigation
German Aerospace Centre (DLR)
Kalkhorstweg 53, 17235 Neustrelitz, GERMANY
email: {michailas.romanovas, luis.lanca, ralf.ziebold}@dlr.de

Abstract: *Although the GPS/GNSS had become the primary source for Position, Navigation and Timing (PNT) information in maritime applications, the ultimate performance of the system can strongly degrade due to space weather events, deliberate interference and overall system failures. Within the presented work the development of an affordable integrated PNT unit for future on-board integrated system is presented. The system serves the task to collect and integrate the data from individual sensors in order to deliver the PNT information with a specified performance according to the requirements of the e-Navigation initiative proposed by the International Maritime Organization (IMO). The paper discusses an ongoing activity of replacing an expensive FOG inertial measurement unit with an affordable MEMS sensor system. Preliminary results of the system performance are presented for both static and dynamic scenarios using an Unscented Kalman filter with unit quaternions for the attitude parametrization.*

1. Introduction

Although the importance of the Position Navigation and Timing (PNT) unit for provision of robust information has been already recognized by the e-Navigation initiative proposed by the International Maritime Organization (IMO), its adoption for smaller size vessels is strongly conditioned on the total ownership costs of the system. In our previous works [2] we have demonstrated the feasibility of the approach for both inland waterways and open sea operations, where high performance inertial sensors such as fiber optic gyroscopes (FOGs) have been used to improve the performance of the Global Navigation Satellite System (GNSS) approach. However, a dramatic progress in performance of lower cost MicroElectroMechanical System (MEMS) sensors had led to an appearance of affordable inertial measurement units (IMUs) of tactical grade. Although the main characteristics of the MEMS sensors are still inferior of those of more expensive FOG-based systems, their accuracy can become sufficient for some application scenarios such as coasting GNSS outages of duration of several seconds while still satisfying the accuracy requirements of maritime applications.

The presented work analyzes the performance of the developed PNT unit where an expensive FOG sensor is replaced by the MEMS-based IMU. The Unscented Kalman Filter (UKF) with

quaternion attitude parametrization is employed to fuse the inertial and GNSS information. The developed system is evaluated by introducing an artificial GNSS outage of prolonged duration and assessing the accuracy of a pure inertial solution while the satellite information is not available. As the performance of modern MEMS IMUs is rapidly improving both in terms of the sensor noise and bias stability, one can expect the overall characteristics of the PNT unit with MEMS sensor to become similar to those of systems based on FOGs already in the nearest future, while maintaining factor 5x-20x price advantage in the costs of the inertial part. Moreover, the MEMS sensor can be also used as redundant component in order to detect certain failure modes.

Although the MEMS inertial sensors have attracted an increasing attention for the pedestrian localization, certain automotive applications or low-cost UAV design, their applicability in safety critical scenarios such as the maritime navigation has been till recent limited mainly by a poor performance of inertial sensors, causing a rapid drift of the standalone inertial solution when the GNSS or other reference position information is not available. Some recent works [9] have also assessed a possibility to replace the FOG with higher performance MEMS IMUs. The authors confirmed that a combined IMU/GNSS system is able to deliver the position and the velocity information at rapid update rate while preserving a low noise content due to smoothing performance of the inertial integration. Moreover, such a system is able to provide an additional warning signal when the inertial output starts to deviate rapidly from the GNSS reference. Unfortunately, as the work [9] is dated 2008, the performance of the MEMS sensors tested was apparently insufficient to ensure an accurate navigation for the outages of 30-60 seconds and the FOGs have been suggested for practical implementation at the time of the study.

Increasingly commercial systems [3] are available which provide an integration of the GNSS with MEMS inertial sensors. Unfortunately, such systems are often based on proprietary algorithms and are carefully tuned with respect to the characteristics of a particular sensor system. Although such units can be often used as an industry level reference, their extension for innovative integrity monitoring schemes is somehow limited due inability to access and modify the fusion algorithms.

2. Methods

The sensor fusion is implemented by formulating a corresponding estimation problem with the process and measurement models given by corresponding strapdown inertial integration and GNSS measurement models. Here for the given stochastic dynamic system a corresponding Recursive Bayesian Estimation (RBE) algorithm is constructed. Here the strategy based on RBE framework allows to combine all relevant information including sensor noise models, kinematic constraints and even meta-information such as operation modes. A generic RBE algorithm cycle is performed in two steps:

Prediction The *a priori* probability is calculated from the last *a posteriori* probability using the process model, which describes the system evolution in time.

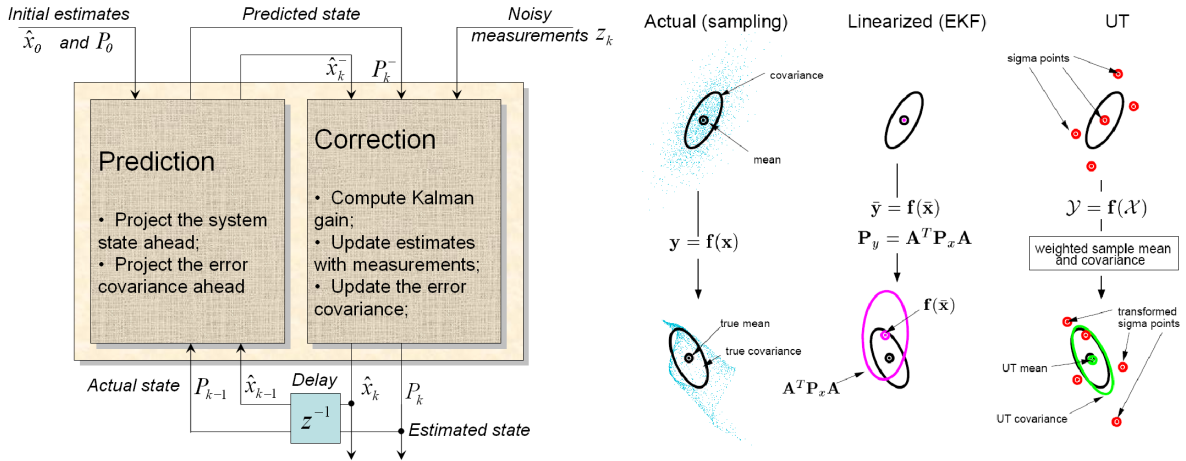


Figure 1: A prediction-correction structure of a classical KF algorithm (left) and the unscented transformation for the mean and covariance propagation [11] (right).

Correction The *a posteriori* probability is calculated from the *a priori* probability using the sensor measurement model and the current measurement z_k .

In practice, however, the methods formulated using the probability distributions do not scale up very well and can quickly become intractable even for problems of relatively modest dimensionality. Various implementations of the RBE algorithms differ in the way the probabilities are represented and transformed in the process and measurement models [10, 6]. If the models are linear and the probabilities are Gaussian, the linear KF is an efficient and optimal solution of the estimation problem. The KF follows a well known prediction-corrections structure is depicted in Fig. 1 (left). Unfortunately, most of the real-world systems are nonlinear and modifications to the linear KF have been developed to deal with the nonlinear dynamics and/or measurement models. The extended KF (EKF) is one of the most popular nonlinear modifications of the LKF and is historically considered as a *de facto* standard within the engineering community. In EKF the nonlinear models are linearized about the current estimate using the Taylor series expansion. The state transition and observation matrices are replaced with the associated Jacobians and similar strategy is used if the process and measurement noises also come in a nonlinear manner. Again, the system at every time t_k is represented by the state x_k and an associated covariance P_k with the rest of the filtering scheme resembling that of the LKF. Although the EKF inherits many advantages of the LKF such as limited computational costs and clear filtering structure, the performance of the estimator strongly depends on the validity of the linearized model assumption and the filter can become inaccurate or even unstable if these assumptions are violated [10].

The UKF is a more recent alternative for the nonlinear estimation problems which uses a deterministic state space sampling instead of the model linearization strategy of the EKF. Here the probability distribution is approximated by a set of deterministically chosen so-called σ -points, which are selected in order to preserve the Gaussian properties of the underlying distribution

under the nonlinear transformation. Each σ -point has two associated weights used for the calculation of the distribution mean and the sample covariance. These σ -points are propagated within the prediction and the correction steps using the direct model formulations while the mean and the covariance of the distribution are calculated back from the weighted sum of these σ -points. The equations of the prediction and correction steps resemble those of the classical KF although reformulated to support σ -points. A detailed description of the algorithm and the associated equations can be found in classical works [7, 11]. An advantage of the UKF can be clearly seen in Fig. 1 (right), where the UKF outperforms the EKF for a model with stronger nonlinearities and results in a distribution closer to the actual one obtained using the Monte Carlo sampling of the state space.

Within the work we employ the unit quaternions for the attitude parametrization. A quaternion is a four dimensional hyper-complex number that is often used to represent the orientation of a rigid body or an associated coordinate frame in a 3D space. Together with the vector counterpart the quaternions provide an alternative approach to homogeneous transformation which can be considered to have certain redundancy due to four trivial numbers [4]. Differently from Euler Angles, the quaternions are not subjected the phenomenon called "gimbal lock", which is an effect preventing the Euler angles to be used when the pitch angle approaches +/- 90 degrees. Yet another alternative attitude parametrization in a form of the rotation matrices results in a difficult renormalization procedure and computational inefficiency (rotation matrix has 9 terms to describe 3D attitude), while the Rodrigues vectors as attitude parametrization do not allow for an easy composition algorithm. Unfortunately, the quaternions have different algebraic properties from the conventional 4D vectors and have to be carefully considered when adopted within the KF.

In order to propagate the attitude noise properly we had implemented a multiplicative UKF [8] which is a combination of two separate versions of the UKF operating either on a more common vector space (position, velocity, ...) with the one for the quaternion part. The unit attitude quaternions are not closed over addition and scalar multiplication which constitute the core of the weighted sum operations within the UKF [1] and the generation of the associated σ -points is implemented by forming a special perturbation quaternion from the rotation vectors, formed from the corresponding components of the process noise covariance matrix. The noise quaternions are calculated from the columns of the square-root of the quaternion part of the covariance matrix. Additionally, some modifications to a classical UKF scheme have to be introduced in the residual calculation as well. Finally the attitude integration is formulated as a quaternion multiplication, where the original attitude quaternion is multiplied by an incremental quaternion formed from the measured angular rate and perturbed with the noise quaternion, associated with the noise of the gyroscope. The multiplicative quaternion propagation leads to a natural way of maintaining the normalization constraint compared to heuristic normalization implemented, e.g. in additive brute-force EKF. The vector part of the UKF follows a classical approach to be found elsewhere [7, 11]. Note that both the gyroscope and the accelerometer outputs are used as noisy control inputs within the associated filter. This strategy not only reduces the dimensionality of the estimation problem, but also also allows to avoid an explicit modeling

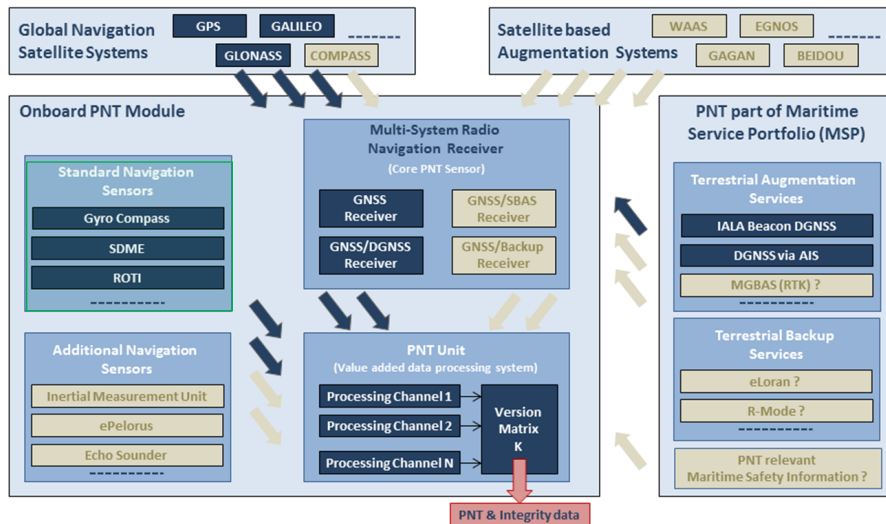


Figure 2: A general concept for the multi-sensor system for the PNT unit.

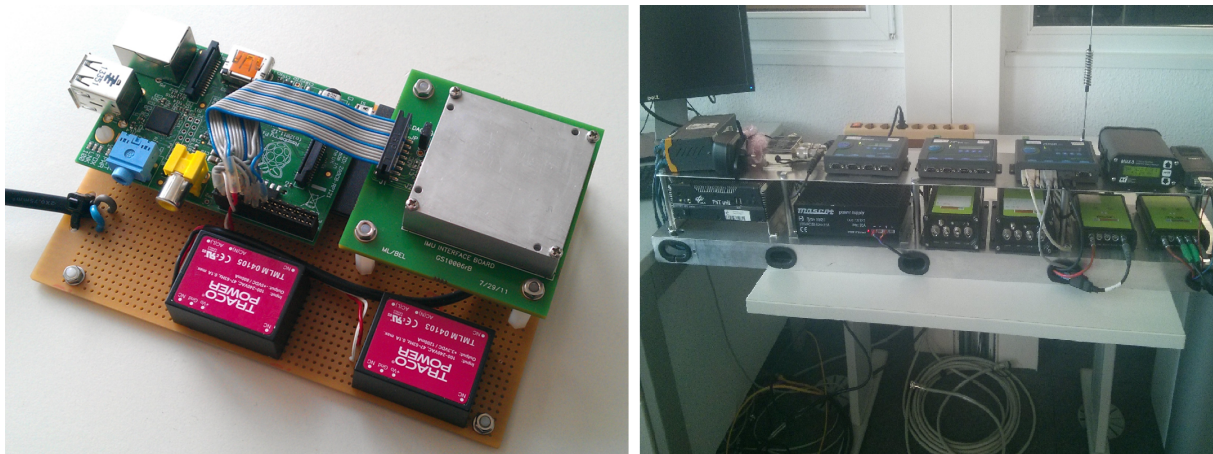


Figure 3: A developed MEMS module using Analog Devices ADIS16485 IMU and ARM-based embedded platform (left) and the GNSS part of the setup in the laboratory (right).

of the motion dynamics.

3. Setup

A general concept of the multi-sensor system for the PNT unit is shown in Fig. 2. Within the presented work we address a particular PNT unit configuration, where the GNSS information is fused with the output of the inertial sensors (accelerometers and gyroscopes). All the sensor data have been pre-processed and logged in real-time (C++, Linux) using a custom developed software running on the PNT unit. The test vessel was equipped with three GNSS antennas and corresponding receivers (Javad Delta, Fig. 3 (left)) as well as a reference high performance

FOG IMU (iMar IVRU FCAI). The developed MEMS module is based on tactical grade Analog Devices ADIS16485 MEMS IMU and is shown in Fig. 3 (right). A commercially available ARM-based platform was adopted to interface the sensor module with the rest of the system. The platform is based on a single-core Broadcom BCM2835 SOC running at 700 MHz with 512 MB RAM and a custom Linux distribution configured with real-time kernel. The readout and pre-processing software is based on the same real-time framework as the main fusion PNT unit (see [5] for details). The interface platform serves several purposes such as SPI-based IMU readout and sensor configuration, TCP/IP data transmission as well as NTP-based synchronization of the module. The latter issue is of a primary importance in order to ensure that MEMS IMU data are properly synchronized and optimally fused with the rest of the sensing modalities. Here an internal time stamp is assigned and redundant information is introduced in order to detect possible packet loss, although no such events have been observed so far during the test runs.

The MEMS IMU consists of 3-axis gyroscope and 3-axis accelerometer as well as an internal temperature sensor with the sensor data readout implemented at 205 Hz. The sensor outputs have 32-bit resolution, although rather minor difference has been observed when using 16-bit or 32-bit sensor configuration. The gyroscope range is 450 dps with reported 6 deg/hr in run bias stability and $0.3 \text{ deg}/\sqrt{h}$ angular random walk. The accelerometer range is fixed to 5g with $32 \mu\text{g}$ in run bias stability and $0.023 \text{ m/s}/\sqrt{h}$ velocity random walk. The performance of the MEMS IMU was checked in laboratory conditions using standard means such as Allan Variance (see Fig. 4) and a correspondence to the manufacturer specification has been found.

Additional sensor information was also made available such as the output of the gyrocompass, a Doppler speed log etc, but these sensor data were not employed within the presented fusion algorithm in order not to obscure the peculiarities of GNSS and IMU integration. Note that the IMU placement is different from the one of GNSS antennas and a level-arm compensation has to be introduced. The results presented in this work are based on the data collected during a normal vessel operation on 01.09.2014 near to the port of Rostock. Within the previous projects, DLR had developed and deployed a Maritime Ground Based Augmentation System (MGBAS) near to the Rostock port. This system allows the position estimation up to decimeter accuracy as well as an accurate monitoring of the GNSS signal quality. Based on the MGBAS as well as the raw data from IGS stations in proximity, the RTK results are generated and used as the reference information within the designed filter when the fix is obtained, while floating solutions are simply ignored [2].

4. Results

Fig. 5 shows the outputs of both inertial sensors during the static scenario. One can clearly see a significant difference in the noise performance for both accelerometer (only Z axis is shown) and the gyroscopes, which comes, however, at no surprise due to the official performance specifications of the sensors. Unfortunately, the outputs of the MEMS sensors also show significant offsets with respect to the reference FOG for both the accelerometer and the gyroscope. Figure

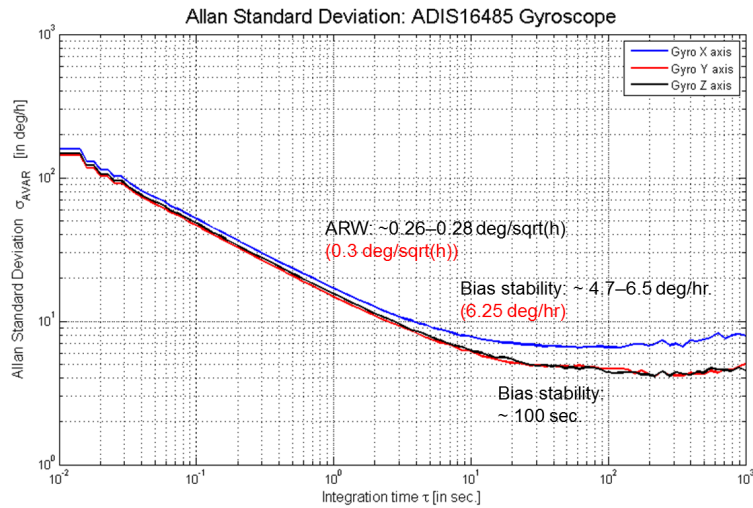


Figure 4: Measured Allan variance of the gyroscopes in ADIS16485.

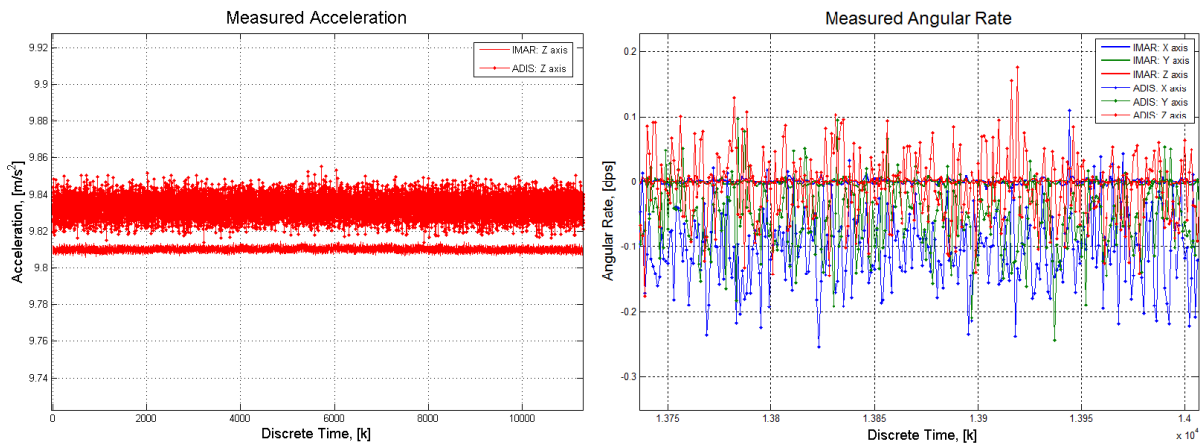


Figure 5: An example of measured acceleration Z component of both MEMS and FOG IMUs (left) and measured gyroscope outputs (right) for static scenarios.

6 shows the initial results of a loosely-coupled IMU/GNSS UKF where the RTK fixes are employed as the reference position measurements. The left figure shows a static scenario where no special GNSS outages are introduced and the RTK position information is provided on their rate of availability. One can clearly see that there is almost no difference between both IMUs as the integration time between the RTK measurements is too short for the differences in drift to become significant. However, at the outage duration of 30 seconds (right figure) prominent drift for both sensor setups can be observed. The drift of the FOG is around 2 meters which can be considered as a reasonable performance, while the drift of the MEMS sensor is already larger than 10 meters under the same conditions.

The results for the dynamic scenario are also shown in Fig. 7, where the outage of 30 seconds

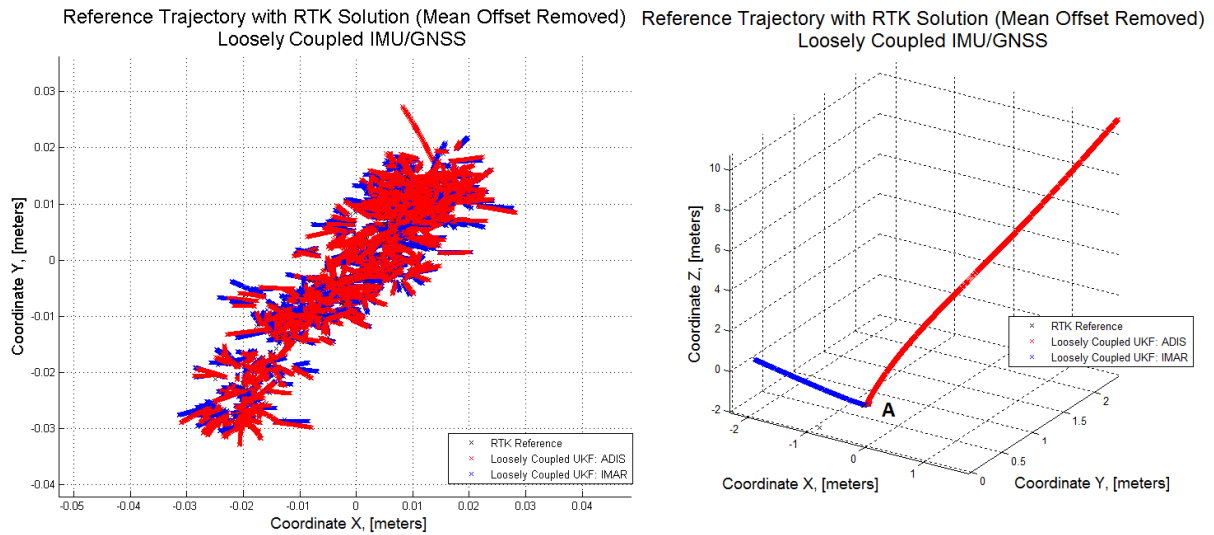


Figure 6: Performance of both IMUs for a static scenario with continuously available RTK fixes (left) and with 30 second imposed outage (right). Region A in the right figure corresponds to a true position as shown in the left figure.

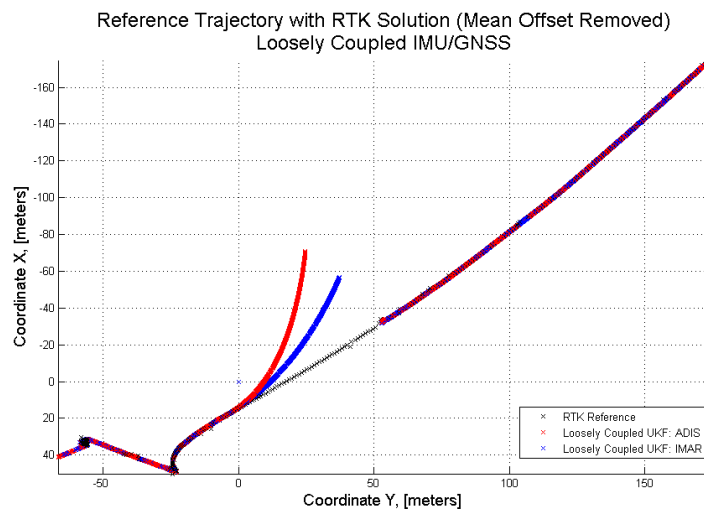


Figure 7: Performance of the filters for a dynamic scenario with a 30 seconds outage imposed on RTK measurements.

is imposed to assess the behavior of the systems at the absence of the reference information. Although the performance of the FOG-based system is better than that of the system with the MEMS sensor, the ultimate difference in terms of the final position drift is only appr. 2x larger for the given trajectory segment and can be considered as reasonably good bearing in mind 20x cost difference between the MEMS and FOG sensors.

5. Discussion

The obtained results confirm that under good calibration conditions the MEMS IMU can provide fairly good performance close to that of the FOG for shorter GNSS outages, although a more expensive FOG could significantly outperform the MEMS sensor for longer outages. Note that in all the cases an estimated gyroscope offset was subtracted from the MEMS IMU before the attitude integration. In reality, when the gyroscope offset is not known, but is estimated within the filter itself, the performance could slightly worsen and would depend on how accurate the actual offset estimation is. Here no special calibration has been performed for the MEMS accelerometer, which could also partially explain slightly worse performance of the ADIS IMU.

Obviously, the MEMS sensor shows an inferior performance when compared to that of an expensive FOG IMU. However, the biggest concern should be not due to the additive noise, present in the sensor output, but rather due to the sensor calibration. Here a fixed offset at the accelerometer output results in a quadratic in time error accumulation, while gyroscope offset leads to a cubic in time drift of the position. Therefore, the MEMS sensor has to be carefully calibrated or a special joint estimation filter has to be constructed, where the sensor offsets and/or other parameters have to be estimated in real-time in parallel with the conventional motion variables. This, however, can be only implemented when an observability of the calibration parameters is verified as any attempt to estimate too many sensor parameters simultaneously could lead to the filter divergence. Moreover, improper sensor calibration can result in much slower convergence of the filter when initialized far from the true state or even divergence if the observation models ensure only local observability of the system.

Conceptually, when used alone for GNSS-only measurements, the KF solution would be not too much different from a classical least-squares solution. When one ignores the cases of lower satellite visibility, the KF-based approaches are, to large extent, the weighted versions of the recursive least square estimators. The fundamental difference between the LS approach and RBE techniques is that KF explicitly assumes some receiver dynamics, formulated as the process model within the RBE algorithm. However, when the process modeling assumptions are incorrect, the problems can arise. Nevertheless, if the process model assumptions are reasonable and match the true receiver dynamics, the KF would perform much better than a memory-less LS solver. Here, however, the IMU solves exactly the dynamics modeling problem as the inertial measurements are integrated directly and provide smooth and continuous state estimation while preserving all the dynamical details.

Although the results above are demonstrated using UKF techniques, the final system will be implemented using more efficient error-state EKF. While having similar performance for the most of navigation applications, the EKF avoids the computational burden of generating the σ -points. An important further step is to include and validate the integrity mechanisms for the KF-based methods using different sensing modalities. Although several mechanisms have been historically proposed for the integrity monitoring within the KFs, so far no widely adopted technique exists suitable for the safety-critical applications. Here one of the main challenges comes due to the internal memory of the RBE algorithms, where an effect of the erroneous

measurement remains, in principle, forever within the estimated state.

6. Conclusions

Within the presented paper we have successfully demonstrated an application of the MEMS IMU within a maritime integrated PNT unit as possible replacement of a far more expensive FOG IMU. The performance of the prototype system has been evaluated using the sensor measurements recorded during the real vessel campaigns. When carefully calibrated, the MEMS sensor is able to bridge the GNSS outages of a reasonable duration and can be considered as a part of a future resilient PNT unit. The approach is consistent with the development of the e-Navigation strategy and, at the same time, results in an affordable setup due to lower costs with a promising potential for performance improvement due to constantly increasing performance of the MEMS sensors.

References

- [1] Yee-Jin Cheon and Jong-Hwan Kim. Unscented filtering in a unit quaternion space for spacecraft attitude estimation. In *Industrial Electronics, 2007. ISIE 2007. IEEE International Symposium on*, pages 66–71, June 2007.
- [2] Zhen Dai, R. Ziebold, A. Born, and E. Engler. Heading-determination using the sensor-fusion based maritime pnt unit. In *Position Location and Navigation Symposium (PLANS), 2012 IEEE/ION*, pages 799–807, April 2012.
- [3] Tom Ford, Jason Hamilton, Mike Bobye, and Laurence Day. GPS/MEMS inertial integration methodology and results. Technical report, NovaTel, 2004.
- [4] J. Funda, R.H. Taylor, and R.P. Paul. On homogeneous transforms, quaternions, and computational efficiency. *Robotics and Automation, IEEE Transactions on*, 6(3):382–388, 1990.
- [5] S. Gewies, C. Becker, and T. Noack. Deterministic framework for parallel real-time processing in gnss applications. In *Satellite Navigation Technologies and European Workshop on GNSS Signals and Signal Processing, (NAVITEC), 2012 6th ESA Workshop on*, pages 1–6, Dec 2012.
- [6] M. S. Grewal and A. P. Andrews. *Kalman Filtering. Theory and Practice using MATLAB, 2nd edition*. John Wiley & Sons, Inc. New York, 2001.
- [7] S.J. Julier and J.K. Uhlmann. Unscented filtering and nonlinear estimation. *Proceedings of the IEEE*, 92(3):401 – 422, March 2004.
- [8] E. Kraft. A quaternion-based unscented Kalman filter for orientation tracking. In *Information Fusion, 2003. Proceedings of the Sixth International Conference of*, volume 1, pages 47–54, July.
- [9] Terry Moore, Chris Hill, Andy Norris, Chris Hide, David Park, and Nick Ward. The potential impact of GNSS/INS integration on maritime navigation. *The Journal of Navigation*, 61:221237, 2008.
- [10] Sebastian Thrun, Wolfram Burgard, and Dieter Fox. *Probabilistic Robotics (Intelligent Robotics and Autonomous Agents)*. The MIT Press, September 2005.
- [11] E.A. Wan and R. Van Der Merwe. The Unscented Kalman filter for nonlinear estimation. In *Adaptive Systems for Signal Processing, Communications, and Control Symposium 2000. AS-SPCC. The IEEE 2000*, pages 153 –158, 2000.